Devil's staircases without particle-hole symmetry

Zhihao Lan, Igor Lesanovsky, and Weibin Li

School of Physics and Astronomy, University of Nottingham, Nottingham NG7 2RD, United Kingdom
and Centre for the Mathematics and Theoretical Physics of Quantum Non-equilibrium Systems,
University of Nottingham, Nottingham NG7 2RD, United Kingdom

We present and analyze spin models with long-range interactions whose ground state features a so-called devil's staircase and where plateaus of the staircase are accessed by varying two-body interactions. This is in contrast to the canonical devil's staircase, for example, occurring in the one-dimensional Ising model with long-range interactions, where typically a single-body chemical potential is varied to scan through the plateaus. These systems, moreover, typically feature a particle-hole symmetry which trivially connects the hole part of the staircase (filling fraction $f \geqslant 1/2$) to its particle part ($f \leqslant 1/2$). Such symmetry is absent in our models and hence the particle sector and the hole sector can be separately controlled, resulting in exotic hybrid staircases.

I. INTRODUCTION

A devil's staircase is a fractal structure that characterizes the ground state of a plethora of systems in physics [1,2]. Examples include the Frenkel-Kontorowa model [3,4], the Falicov-Kimball model [5–7], Ising models [8,9], quantum dimer models [10–12], as well as certain discrete maps [13–15]. In particular, one-dimensional (1D) Ising models are paradigmatic systems that may exhibit devil's staircases both in the case of long-range and short-range interactions. In Ising models with long-range interactions it was shown rigorously that the permitted filling fractions (ratio of the number of particles to that of lattice sites) of the ground-state configurations form a complete devil's staircase when the chemical potential is varied [8]. This means when scanning the chemical potential, the filling fractions can assume all rational numbers. For the short-range interacting anisotropic next-nearest-neighbor Ising (ANNNI) model, such a staircase appears only at finite temperatures [9] since there are solely two stable ground states (known as the ferromagnetic phase and antiphase) at zero temperature. The staircase structure of the ANNNI model has been observed in NaV_2O_5 under high pressure [16].

In recent years, controllable quantum systems have emerged as platforms for exploring phenomena in condensed-matter and high-energy physics [17]. This includes trapped ions [18,19], cold polar molecules [20–24] and strongly interacting Rydberg atoms [25–30], ultracold atoms in bichromatic lattices [31], synthetic dimensions and gauge fields [32], photons with engineered long-range interactions [33], and optomechanical cavity systems [34]. These platforms allow one not only to control single-body quantities (e.g., the trapping potential or the chemical potential), but also to tailor the shape of the underlying two-body interaction.

In a recent study [35], we have identified a new mechanism underlying the formation of a devil's staircase within a spin model implemented by Rydberg atoms held in a 1D optical lattice. By using a so-called double-dressing scheme [35],

we have shown how to create competing interactions with short-range attraction and longer-range repulsion between two atoms. In particular, we focused on a situation where the nearest-neighbor interaction is attractive and tunable while the interactions from next-nearest neighbors onwards follow a repulsive van der Waals (vdW) potential. Such a nonconvex potential leads to the formation of a devil's staircase in the ground state and its plateaus are accessed by varying the strength of the nearest-neighbor attraction.

This situation is in contrast to that encountered, e.g., in the above-mentioned staircase of the Ising model, which is governed by a single-body chemical potential term. The staircase in the Ising model features a particle-hole symmetry, i.e., the hole part of the staircase at filling fraction $f \geqslant 1/2$ can be trivially extracted from the particle part of the staircase at $f \leqslant 1/2$. In our previous work [35], we have shown that a broken particle-hole symmetry emerges for a staircase whose plateaus are accessed by two-body attractive interactions. In this situation the staircase is a union of two substaircases that are consisting of either dimer particles or dimer holes. This finding opens up the possibility to study a plethora of hybrid staircases. For example, it is possible to encounter a situation with a dimer-particle substaircase in the particle sector and a trimer-hole substaircase in the hole sector. Finally, we would like to note that the impact of different kinds of interactions on the devil's staircase physics has been studied in the literature from different perspectives [36–43]. For example, some aspects of the staircases discussed in the present work can be linked to studies of atoms adsorbed on a surface [38,40]. However, a systematic exploration of devil's staircases from the perspective of particle-hole symmetry breaking has not been conducted previously.

In this paper, we extend our previous study [35] to spin models that feature attractive interactions not only among nearest neighbors but over a longer range. The paper is structured as follows: In Sec. II, we present the model Hamiltonian and discuss the role played by the particle-hole symmetry. In Sec. III, we discuss analytical and numerical tools for analyzing
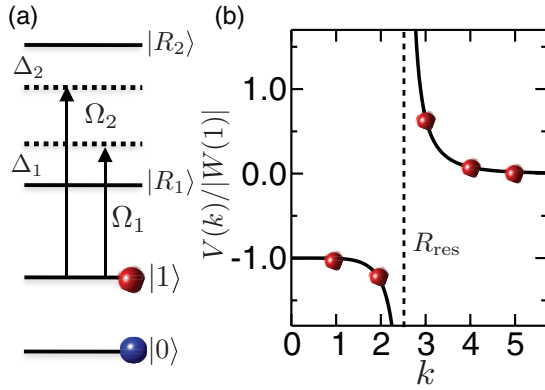
FIG. 1. (a) Level scheme. An electronically low-lying state $|1\rangle$ is laser coupled to Rydberg states $|R_1\rangle$ and $|R_2\rangle$ with Rabi frequency Ω_1 and Ω_2, and detuning Δ_1 and Δ_2, respectively. (b) Effective interaction potential between particles in dressed state $|1\rangle$. This interaction is attractive at short distances and repulsive at long distances. Here, we show a situation where the nearest neighbor and next-nearest neighbor are attractive, i.e., $W(1) < 0$ and $W(2) < 0$.

the ground-state properties of the model Hamiltonian. In Sec. IV, we benchmark our tools by applying them to a conventional staircase controlled by a chemical potential. In Sec. V, we investigate in detail the situation where two-body interactions drive staircases without particle-hole symmetry, which constitutes the central part of this work. In Sec. VI, we discuss the possibility of staircases controlled by n-body interactions ($n > 2$). We conclude and provide an outlook in Sec. VII.

II. MODEL HAMILTONIAN

Staircases explored in this work rely on a nonconvex long-range interaction which is attractive at short distances and repulsive at large distances. In our previous work [35], we proposed that a special form of this interaction, i.e., with van der Waals repulsive tail, can be engineered with the help of Rydberg atoms. Specifically, the physical setting is a 1D lattice with spacing a where each site can either be occupied by an atom in state $|1\rangle$ or $|0\rangle$. For convenience, we denote that a site is empty (occupied by a particle) when the atom of the site is in state $|0\rangle$ ($|1\rangle$). We then employ a double-dressing scheme [35], in which two blue- and red-detuned lasers are applied simultaneously to weakly couple the $|1\rangle$ state with two Rydberg S states $|R_1\rangle$ and $|R_2\rangle$, as depicted in Fig. 1(a). The Rabi frequency and detuning of the blue-(red-) detuned laser are Ω_1 (Ω_2) and Δ_1 (Δ_2), respectively. The vdW interaction of the Rydberg state $|R_j\rangle$ is C_j/r^6, with C_j the corresponding dispersion constant ($j = 1,2$). We will neglect the interstate Rydberg interaction when the two states are far separated energetically [44]. The lasers induce long-range interactions between atoms in the Rydberg dressed $|1\rangle$ state [45–48]. The blue-detuned laser induces an interaction potential $U_1(r) = \tilde{C}_1/(r^6 - R_{\rm res}^6)$, where $\tilde{C}_1 = R_{\rm res}^6 \Omega_1^4/8\Delta_1^3$ and $R_{\rm res} = (C_1/2|\Delta_1|)^{1/6}$ determines the distance of the two-atom resonant excitation when $2\Delta_1 + C_1/R_{\rm res}^6 = 0$ [49,50]. The resulting interaction is attractive for $r < R_{\rm res}$ and repulsive when $r > R_{\rm res}$. The red-detuned laser generates a

lon-range soft-core interaction $U_2(r) = \tilde{C}_2/(r^6 + r_2^6)$, where $\tilde{C}_2 = r_2^6 \Omega_2^4/8\Delta_2^3$ and the core radius $r_2 = (C_2/2|\Delta_2|)^{1/6}$. The overall dressed interaction is given by the combined potential of $V(r) = U_1(r) + U_2(r)$, which is illustrated in Fig. 1(b). By tuning the laser parameters, the strength and attractive range of the nonconvex long-range two-body interactions can be varied (details of the implementation are given in Ref. [35]).

In this paper, we will go beyond this special realization with Rydberg atoms and consider more general nonconvex interactions, where the repulsive tail is not limited by the vdW type, i.e., $V(r) \sim 1/r^\alpha$ with $1 < \alpha$, focusing more on the physics rather than the experimental implementations. When α is taken as a parameter that can be freely tuned, many different features are found in the respective staircase which are not revealed using the vdW interaction. Taking these considerations into account, we study a classical 1D spin chain governed by the following Hamiltonian,

$$H = \sum_{i=-\infty}^{\infty} \sum_{r=R+1}^{\infty} V(r)n_i n_{i+r} + \sum_{i=-\infty}^{\infty} \sum_{r=1}^{R} W(r)n_i n_{i+r}, \quad (1)$$

where $W(r) \leqslant 0$ ($r = 1, \ldots, R$) parametrizes the strength of the attractive potential part, with R to be the range of the attractive interaction. The potential $V(r) = (R+1)^\alpha/r^\alpha$ ($r = R+1, \ldots$) corresponds to the repulsive tail. Note that here and in the following, the energy is expressed in units of $V(R+1)$ and length in units of the lattice spacing a.

A particle-hole symmetry is absent in Hamiltonian (1), which is explicitly seen by applying the particle-hole transformation $n_i = 1 - m_i$, where m_i denotes the occupation of a hole at the ith site. This yields the Hamiltonian for the holes,

$$H = \sum_{i=-\infty}^{\infty} \sum_{r=R+1}^{\infty} V(r)m_i m_{i+r} + \sum_{i=-\infty}^{\infty} \sum_{r=1}^{R} W(r)m_i m_{i+r}$$
$$- \mu' \sum_{i=-\infty}^{\infty} m_i + C, \quad (2)$$

where $\mu' = 2\sum_{r=R+1}^{\infty} V(r) + 2\sum_{r=1}^{R} W(r)$ and $C = \sum_{i=-\infty}^{\infty} \sum_{r=R+1}^{\infty} V(r) + \sum_{i=-\infty}^{\infty} \sum_{r=1}^{R} W(r)$. The extra μ' term, which is controlled by interactions $V(r)$ and $W(r)$, is typically nonzero. In this case, the Hamiltonian of the hole is structurally different from that of the particle.

III. METHODS

To investigate the ground state of Hamiltonian (1), we will use both analytical and numerical tools. The analytical method is based on that by Bak and Bruinsma [8]. It was originally used to deal with repulsive and convex interactions and we will adapt it to our system. The analytic treatment is accompanied by "brute-force" numerical calculations to find the ground state of (1).

A. Analytical method

1. Stability regions of monomers

When studying the Ising model with convex interactions, Bak and Bruinsma [8] showed that for any rational filing fraction $f = \frac{q}{p}$ (p and q are non-negative integers) of the

particles to the lattice sites, there will be a finite range, i.e., a stability region of chemical potential (with lower and upper bound μ^- and μ^+, respectively), such that the most homogeneous configuration with this filling fraction is the ground-state configuration.

The stability regions are determined by the following equations (the derivation is for convenience given in Appendix A),

$$
\mu^- = \sum_{n=1,\alpha_n \neq 0}^{\infty} [(r_n + 1)V(r_n) - r_n V(r_n + 1)]
$$
$$
+ \sum_{n=1,\alpha_n = 0}^{\infty} [(r_n + 1)V(r_n) - r_n V(r_n + 1)] \quad (3)
$$

and

$$
\mu^+ = \sum_{n=1,\alpha_n \neq 0}^{\infty} [(r_n + 1)V(r_n) - r_n V(r_n + 1)]
$$
$$
+ \sum_{n=1,\alpha_n = 0}^{\infty} [(-r_n + 1)V(r_n) + r_n V(r_n - 1)], \quad (4)
$$

where r_n and α_n are related to p and q through the relation $np = r_n q + \alpha_n$ with $0 \leqslant \alpha_n < q$. From these equations, we obtain the "width" of the stability region,

$$
\Delta_\mu = \mu^+ - \mu^-
$$
$$
= \sum_{n=1,\alpha_n = 0}^{\infty} [r_n V(r_n - 1) - 2r_n V(r_n) + r_n V(r_n + 1)].
$$
$$
(5)
$$

2. Effective interaction between two n-mer particles and holes

In our case particles tend to form clusters due to the short-range attraction. In general, if the first R nearest-neighbor interactions are attractive, then $R + 1$ particles will form a cluster on sites $(i, i + 1, \ldots, i + R)$. We will refer to such an n-particle (hole) cluster as an n-mer particle (hole).

The method by Bak and Bruinsma is extended to capture this case by treating an n-mer as an effective "monomer." To this end, one needs to know the effective chemical potential for an n-mer and the interaction between two n-mers. (Note that, for an n-mer with filling fraction q/p, the corresponding filling fraction of the actual monomers is nq/p.) The interaction between two n-mer particles (holes) separated by r lattice sites, as shown in Fig. 2, can be conveniently described by a matrix

$$
\tilde{V} = \begin{pmatrix} V(r) & V(r+1) & \cdots & V(r+n-1) \\ V(r-1) & V(r) & \cdots & V(r+n-2) \\ \vdots & \vdots & \ddots & \vdots \\ V(r-n+1) & V(r-n+2) & \cdots & V(r) \end{pmatrix},
$$
$$
(6)
$$

where matrix element $\tilde{V}_{ij}$ describes the interaction between the ith particle of the first n-mer and the jth particle of the second n-mer. The effective interaction between two n-mers is then given by $\tilde{V}_{\text{eff}}(r) = \sum_{ij} \tilde{V}_{ij}$. Under the condition that there is no overlap of two n-mers in the most homogeneous configuration, we can use the method by Bak and Bruinsma to describe the n-mers, when we replace the interaction of
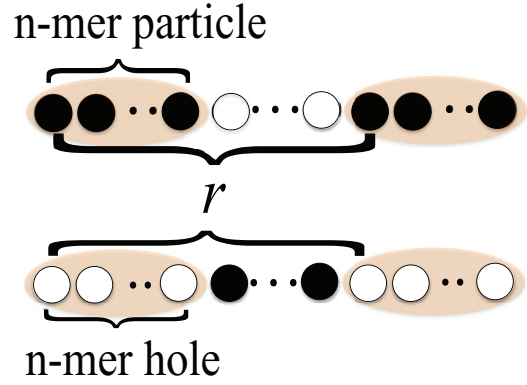

FIG. 2. Two n-mer particles (holes) separated by distance r will interact according to the $2n$ binary interactions of their constituent particles (holes), resulting in the interaction matrix given by Eq. (6).

Eqs. (3)–(5) by $\tilde{V}_{\text{eff}}(r)$. Furthermore, we need to replace the monomer chemical potential by that of the n-mer particle or hole, which will be discussed in the following.

3. Effective chemical potential of n-mer particle and hole

In the case of the n-mer particle, we find that n particles will cluster together to lower their energy when the range of the attractive interactions is $R = n - 1$. According to Hamiltonian (1), the interaction energy within the n-mer particle then serves as an effective chemical potential given by

$$
\mu_{np} = W(n-1) + 2W(n-2) + \cdots + (n-1)W(1). \quad (7)
$$

Note that if $W(i) = W$ for all i, then $\mu_n^p = n(n-1)W/2$.

For an m-mer hole, the calculation of the effective chemical potential is more involved as the size of the hole cluster can be larger than the range of the attractive interactions. Using Hamiltonian (2), we find the effective chemical potential of an m-mer hole,

$$
\mu_{mh}^{(R)} = -E_{mh}^{(R)} = -\sum_{j=1}^{R}(m-j)W(j) - \sum_{k=R+1}^{m-1}(m-k)V(k)
$$
$$
+ 2m \sum_{r=R+1}^{\infty} V(r) + 2m \sum_{r=1}^{R} W(r). \quad (8)
$$

When $m \geqslant R + 1$, the size m depends on both R and the long-range repulsive tail. This is a manifestation of the particle-hole symmetry breaking, i.e., the size of the hole cluster is not necessarily the same as the particle cluster which would give $m = R + 1$. In the following, we list explicitly the effective chemical potentials of particle and hole clusters of different sizes for $R = 1$ and $R = 2$, which are relevant for our discussions below.

$R = 1$: The chemical potentials of particle and hole dimers, and hole trimers are given by

$$
\mu_{2p} = W(1), \quad (9)
$$

$$
\mu_{2h}^{(1)} = 4 \sum_{r=2}^{\infty} V(r) + 3W(1), \quad (10)
$$

$$
\mu_{3h}^{(1)} = 6 \sum_{r=2}^{\infty} V(r) - V(2) + 4W(1). \quad (11)
$$

$R = 2$: The chemical potentials of particle and hole trimers, and hole tetramers are given by

$$\mu_{3p} = W(2) + 2W(1), \tag{12}$$

$$\mu_{3h}^{(2)} = 6\sum_{r=3}^{\infty} V(r) + 4W(1) + 5W(2), \tag{13}$$

$$\mu_{4h}^{(2)} = 8\sum_{r=3}^{\infty} V(r) - V(3) + 5W(1) + 6W(2). \tag{14}$$

In order to obtain the stability regions of n-mer particles and holes [for Hamiltonians (1) and (2)], we can now use Eqs. (3)–(5) with the effective interaction $\tilde{V}_{\mathrm{eff}}(r)$, the effective chemical potentials μ_{np} and $\mu_{nh}^{(R)}$, as well as the true monomer filling fraction nq/p (associated with an n-mer particle) or hole filling fraction q/p.

The above effective theory for n-mer particles and holes only works when the staircase contains no mixtures of n-mers of different kinds. The aim of this work is to understand when the staircase can be described by a union of two pure substaircases in the particle and hole sectors, respectively.

B. Numerical method

The filling fractions associated with the ground-state configuration of Hamiltonian (1) as functions of the attractive interaction $W(r)$ ($r = 1, 2, \ldots, R$) can be calculated by a brute-force method. In this numerical method [35], we check all possible periodic configurations of an infinite chain with period p up to a certain limit ($p = 23$ in this study, due to the limitation of computational resources). The ground-state configuration is determined by the one that has the lowest-energy density (energy of a single period divided by the length of the periodicity). This captures the coarse structure of the staircase as the phases with large p usually have very small [1] stability regions.

IV. PARTICLE-HOLE SYMMETRY IN TRADITIONAL DEVIL'S STAIRCASES

To provide some context, we review here briefly the results by Bak and Bruinsma [8], which are based on an Ising model with long-range interactions,

$$H = \sum_{i=-\infty}^{\infty} \sum_{r=1}^{\infty} V(r) n_i n_{i+r} - \mu \sum_{i=-\infty}^{\infty} n_i, \tag{15}$$

where $n_i = 0, 1$ when the site i is empty or occupied by a particle, respectively. Here, $V(r)$ describes a long-range repulsive interaction between two particles separated by r sites and μ is the chemical potential for the particle. For any rational filling fraction f of the particles, the ground-state configuration will assume a distribution in space as uniform as possible if the infinite-range interaction $V(r)$ is strictly convex [51,52]. In this case the ground-state configuration is independent of the actual details of the interaction potential and features so-called generalized Wigner crystals. The filling fractions f of the ground-state configurations form a complete devil's staircase as a function of the chemical potential μ [8].
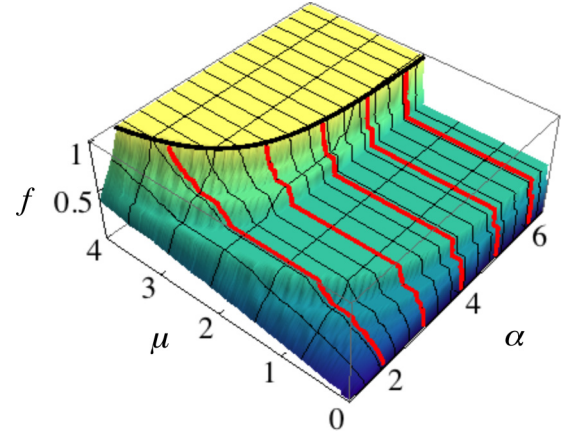

FIG. 3. Ground-state filling fractions f of Hamiltonian (15) as functions of the chemical potential μ and the power α of the power-law interaction potential. The large plateau at half filling, $f = 1/2$, corresponds to the configuration of $101010\ldots$. The red solid lines are analytical results obtained from Eqs. (3) and (4) at $\alpha = 2, 3, 4, 5$, and 6. The black line is the critical chemical potential $\mu_c(\alpha) = 2\zeta(\alpha)$ at which the ground states of Hamiltonian (15) turn into the fully filled particle states with $f = 1$.

For power-law interactions $V(r) = 1/r^{\alpha}$, the Hamiltonian (15) is invariant (apart from an irrelevant constant term) under the particle-hole transformation $n_i = 1 - m_i$ and the corresponding hole Hamiltonian reads

$$H = \sum_{i=-\infty}^{\infty} \sum_{r=1}^{\infty} V(r) m_i m_{i+r} - \mu' \sum_{i=-\infty}^{\infty} m_i + C, \tag{16}$$

where $\mu' = 2\sum_{r=1}^{\infty} V(r) - \mu$ and $C = \sum_{i=-\infty}^{\infty} \sum_{r=1}^{\infty} V(r) - \mu \sum_{i=-\infty}^{\infty}$. One can find the transition point to the state without holes (or a state where the lattice is fully occupied by particles) by setting $\mu' = 0$, i.e., $\mu = 2\sum_{r=1}^{\infty} V(r)$. For power-law interactions, the corresponding critical chemical potential μ_c is determined by $\mu_c = 2\zeta(\alpha)$, with $\zeta(\alpha) = \sum_{n=1}^{\infty} 1/n^{\alpha}$ being the Riemann zeta function.

We numerically obtain the staircase structure by varying both the power α of the repulsive power-law interaction and the chemical potential. The result is shown in Fig. 3, which has a "devil's terrace" structure. The big plateau at filling fraction $f = 1/2$ corresponds to a configuration of $101010\ldots$. Its width increases as α increases since the large commensurate phases (with large p) occupy a negligible parameter space of μ due to the fast decaying property of $1/r^{\alpha}$ at large α. At small α, the large commensurate phases play important roles and occupy a large portion of the parameter space of μ.

When $f \leqslant 1/2$, particles in the lattice are all separated from each other by empty sites and there is no cluster behavior of the particles. However, when $f > 1/2$, particles will cluster together to form different kinds of n-mers ($n \geqslant 2$). In this regime, it becomes convenient to instead use the hole Hamiltonian (16). The hole sector at $f \geqslant 1/2$ is trivially related to the particle sector at $f \leqslant 1/2$ as the staircases (e.g., the red lines of Fig. 3) are symmetric around $f = 1/2$ along the μ direction [8]. When the chemical potential of the particles is zero, the ground-state configuration would have no particles in it and, similarly, if the chemical potential of the holes is zero, one would have

no holes in the lattice, i.e., the transition point to a fully filled particle state with $f = 1$ can be obtained by setting the hole chemical potential to zero. This allows us to derive the critical chemical potential analytically, $\mu_c(\alpha) = 2\zeta(\alpha)$. The analytical result (marked by the black curve in Fig. 3) agrees with the numerical calculation. In the same figure, we also present the analytical result from Eqs. (3) and (4) at $\alpha = 2, 3, 4, 5,$ and 6 on top of the numerical data in red lines, which agree with each other very well.

V. TWO-BODY INTERACTION DRIVEN STAIRCASES WITHOUT PARTICLE-HOLE SYMMETRY

In this section we turn to the discussion of devil's staircases corresponding to the ground state of Hamiltonian (1). We will mainly focus on two aspects of the problem. First, we would like to understand how the range of the attraction R changes the structure of the devil's staircases. Second, we investigate the effect of the power α of the interaction potential $V(r) = (R + 1)^\alpha / r^\alpha$. For simplicity, we will consider the case where the short-range attraction $W(i)\,(i = 1, \ldots, R)$ are the same and equal to W.

In particular, we find that the feature of the staircase nontrivially depends on α. For certain α, the staircase can be described by a union of two pure substaircases, i.e., a pure $(R + 1)$-mer particle substaircase and a pure $(R + 1)$-mer or $(R + 2)$-mer hole substaircase. For other values of α, the staircases consist of more than two kinds of basic building blocks.

We use an "complexity parameter" $\mathscr{P}$ to describe this effect. When the value of α is such that the whole staircase can be described by two pure substaircases (a pure n-mer particle substaircase and a pure m-mer hole substaircase), i.e., a single pair of integers (n,m) is sufficient to describe the emergent staircase, then $\mathscr{P}(\alpha) = 1$, otherwise $\mathscr{P}(\alpha) = 0$, which indicates the emergence of more complicated structures. In the following, we will study the staircases of Hamiltonian (1) by considering $R = 1$ and $R = 2$. A general description of $R \geqslant 3$ based on the data at $R = 3, 4, 5,$ and 6 will also be presented.

A. $R = 1$

When the range of the attraction is $R = 1$, only the nearest-neighbor interaction is attractive and the interactions from next-nearest neighbor onwards ($r = 2, \ldots$) are repulsive and follow the form $V(r) = 2^\alpha / r^\alpha$. The case of $\alpha = 6$, corresponding to the van der Waals interaction, has been studied in detail by us in a recent work [35] based on a concrete system of Rydberg atoms. We found that the staircase structure has a dimer-particle substaircase with $f \leqslant 1/2$ and a dimer-hole substaircase with $f \geqslant 1/2$, as shown in Fig. 4(a). The broken particle-hole symmetry in this case does not manifest in the different sizes of the clusters in the two sectors, but rather in the asymmetric shape of the staircase along the W direction in the vicinity of $f = 1/2$. There is no symmetry around $f = 1/2$ and the relative width of certain plateaus can change significantly as we increase α. For example, the plateau corresponding to $f = 1/2$ ($f = 2/5$) becomes very narrow (wide) around $\alpha = 4$, as can be seen in Fig. 4. Such a feature is not found in the Ising model studied by Bak and Bruinsma.
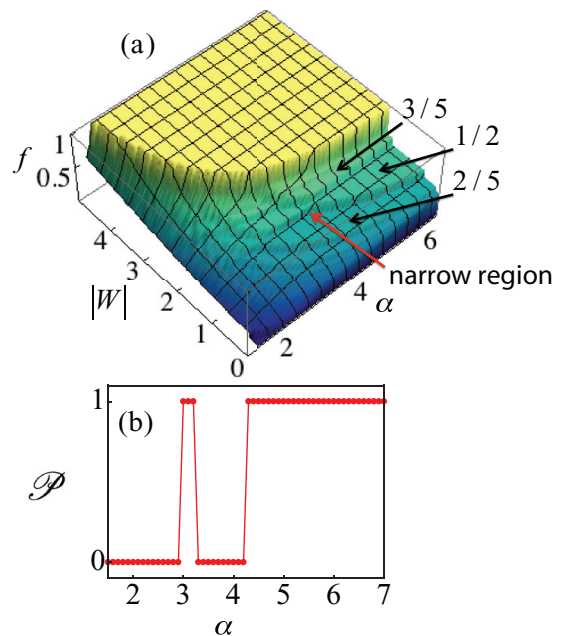

FIG. 4. (a) Ground-state filling fraction f of Hamiltonian (1) at $R = 1$ as functions of the nearest-neighbor attraction W and the power α of the long-range tail of the potential. (b) The complexity parameter $\mathscr{P}(\alpha)$. Only when $\mathscr{P}(\alpha) = 1$, the staircase is described by a union of two pure substaircases. Dots are numerical data and the line is used to guide the eye.

Our next goal is to understand the dependence of the staircases on the interaction exponent α. The complexity parameter $\mathscr{P}(\alpha)$ shows two regions where the staircases can be described by two pure substaircases. One region is $\alpha > 4.2$ and another is around $\alpha = 3$, as shown in Fig. 4(b). When $\alpha > 4.2$, the staircase can be described by two pure substaircases, i.e., a dimer-particle substaircase at $f \leqslant 1/2$ and a dimer-hole substaircase at $f \geqslant 1/2$ [a representative case of $\alpha = 5$ is shown in Fig. 5(a)]. The two substaircases meet at $f = 1/2$ with a configuration of $11001100\ldots$. Decreasing α in this regime narrows this central plateau (at $f = 1/2$) up to $\alpha \approx 4.2$, where it disappears.

Around $\alpha = 3$, we find the staircase consists of a dimer-particle substaircase in the sector of $f \leqslant 2/5$ and a trimer-hole substaircase in the sector of $f \geqslant 2/5$ [see Fig. 5(c) for an example with $\alpha = 3$]. This is intriguing, and is a different manifestation of the particle-hole symmetry breaking. Decreasing α in this regime, the central plateau at $f = 2/5$ becomes narrow up to the point where it completely disappears. As shown in the figure, we do not find other regimes where the staircase can be described by two pure substaircases.

When the hole sector can be described by a single kind of cluster hole, a simple analytic calculation of the phase boundary is possible. For example, in the regime of $\alpha > 4.2$, the hole sector can be solely described by dimer holes, and one can find the exact transition point to the fully filled $f = 1$ particle state by setting the dimer-hole chemical potential [Eq. (10)] to zero, which leads to

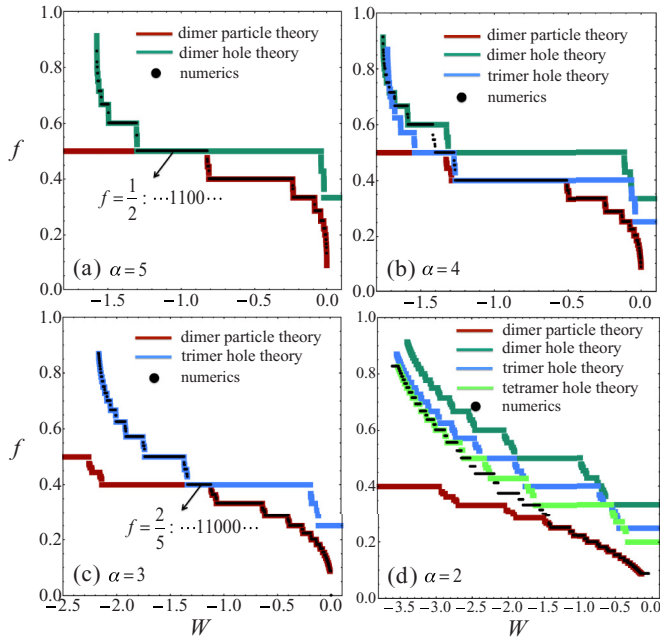$$W_c = -\frac{4}{3} \sum_{r=2}^{\infty} V(r) = -\frac{4[\zeta(\alpha) - 1]2^\alpha}{3}. \qquad (17)$$

FIG. 5. Comparison between analytically and numerically calculated staircases at $\alpha = 2, 3, 4, 5$ as shown in Fig. 4. At $\alpha = 3$ and 5, the staircase can be described by a union of two pure substaircases in both the particle and the hole sectors with $\mathscr{P} = 1$. The case of $\alpha = 5$ is similar to that of our previous work [35] where we considered $\alpha = 6$. At $\alpha = 3$, we find a dimer-particle substaircase and a trimer-hole substaircase which meet at $f = 2/5$ with the ground-state configuration of $1100011000\ldots$. At $\alpha = 2$ and 4, the staircases at the hole sector contain n-mer holes of different kinds.

Similarly, for the regime around $\alpha = 3$, the hole sector can be described by trimer holes. From Eq. (11) we obtain then the transition point,

$$W_c = -\frac{6\sum_{r=2}^{\infty}V(r) - V(2)}{4} = -\frac{6[\zeta(\alpha) - 1]2^{\alpha} - 1}{4}.$$
(18)

For other values of α, the staircase has more complicated structures. Examples with $\alpha = 2$ and 4 are shown in Figs. 5(b) and 5(d), where one cannot describe the emergent staircase with a union of two pure substaircases. For example, we list the ground-state configurations at $\alpha = 4$ for two different W,

$$W = -1.27 \rightarrow 11100011000\ldots f = \frac{5}{11},$$
(19)

$$W = -1.41 \rightarrow 11100111000\ldots f = \frac{6}{11},$$
(20)

which clearly shows that the staircase consists of dimer particles, trimer particles and dimer holes, and trimer holes.

B. $R = 2$

We will now consider the case $R = 2$, i.e., where the attractive range of the interaction potential spans two sites. For simplicity, we will focus on the case where $W(1) = W(2) = W < 0$. The long-range repulsive interaction tail now becomes $V(r) = 3^{\alpha}/r^{\alpha}$ $(r = 3, \ldots)$. For such interactions,
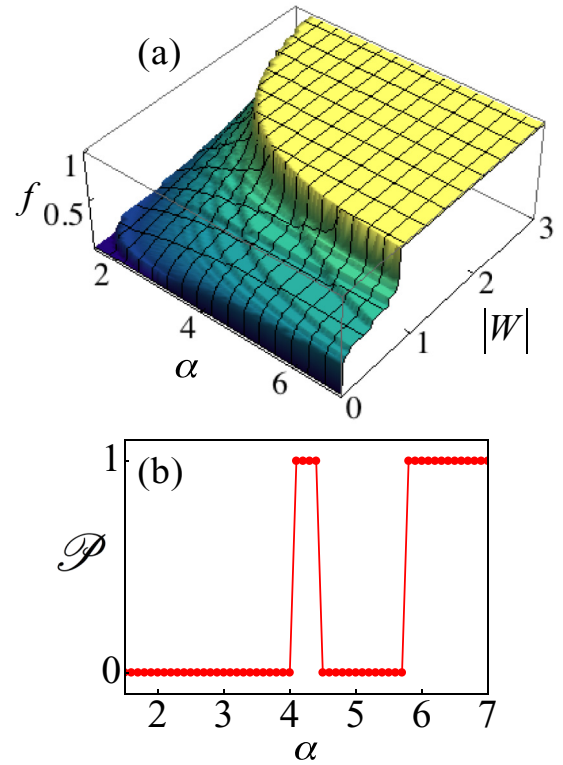

FIG. 6. (a) Ground-state filling fraction f for $R = 2$ as functions of the attractive interaction strength W and the power α. (b) The complexity parameter $\mathscr{P}(\alpha)$. See also Fig. 4.

three particles tend to cluster together on neighboring lattice sites, to form a trimer particle serving as the basic building block of the staircase at the particle sector. The ground-state filling fraction f of Hamiltonian (1) at $R = 2$ is shown in Fig. 6(a).

There are again two regimes where the staircase can be described by a union of two pure substaircases both in the particle and hole sectors, as shown by the complexity parameter $\mathscr{P}(\alpha)$ in Fig. 6(b). When $\alpha > 5.8$, the staircase can be described by a union of a trimer-particle substaircase in the particle sector and a trimer-hole substaircase in the hole sector, where the two substaircases meet at $f = 1/2$ with a configuration $111000111000\ldots$. Around $\alpha = 4.2$, we obtain a trimer-particle substaircase in the particle sector and a tetramer-hole substaircase in the hole sector, where the two substaircases meet at $f = 3/7$ with a configuration $11100001110000\ldots$. Apart from these two regimes, the staircases cannot be described as a union of two pure substaircases. The detailed results of the staircases at $\alpha = 3, 4.2, 5$, and 6 are presented in Fig. 7.

We can also find the exact transition points to the unit filling $f = 1$ particle states in the two regimes where the staircases can be described by a single kind of cluster hole in the hole sector. This is done by setting the trimer-hole and tetramer-hole chemical potentials of Eqs. (13) and (14) to zero, which yields

$$W_c = -\frac{2}{3}\sum_{r=3}^{\infty}V(r) = -\frac{2[\zeta(\alpha) - 1 - \frac{1}{2^{\alpha}}]3^{\alpha}}{3}$$
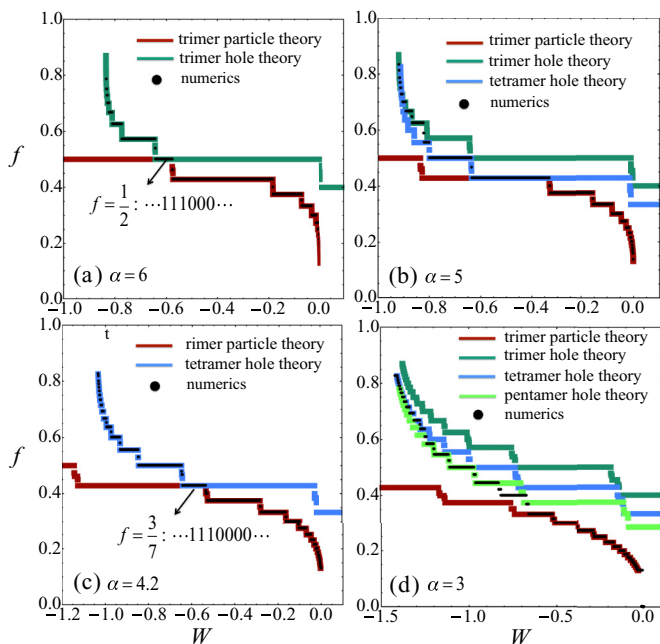(21)

FIG. 7. Analytically calculated staircases compared to the numerically obtained staircases at $\alpha = 6$, 5, 4.2, and 3 in (a)–(d), respectively. The other parameters are $R = 2$ and $W(1) = W(2) = W$. See also Fig. 5.

and

$$W_c = -\frac{8 \sum_{r=3}^{\infty} V(r) - V(3)}{11} = -\frac{8[\zeta(\alpha) - 1 - \frac{1}{2^{\alpha}}]3^{\alpha}}{11}.$$

$$(22)$$

C. $R > 2$

When $R > 2$, the qualitative feature of the physics is largely similar to the case $R = 1$ and $R = 2$. The substaircase in the particle sector is built up from $(R + 1)$-mer particles. In the hole sector, there are two regimes where the staircase can be described by a union of two pure substaircases in both the particle and the hole sectors. In one region, we have an $(R + 1)$-mer particle substaircase and an $(R + 1)$-mer hole substaircase, where the two substaircases meet at $f = 1/2$ with a configuration of $1 \ldots 10 \ldots 0 \ldots$ (with both $R + 1$ "1"s and $R + 1$ "0"s). There is also a narrow region of α, where the staircase is made of an $(R + 1)$-mer particle substaircase and an $(R + 2)$-mer hole substaircase, where the two substaircases meet at $f = (R + 1)/(2R + 3)$ with a configuration of $1 \ldots 10 \ldots 0 \ldots$ (i.e., $R + 1$ particles and $R + 2$ holes). Apart from these two regimes, the staircases cannot be described by a union of two pure substaircases. These features can be seen from the ground-state filling fraction f and order parameter $\mathscr{P}(\alpha)$ of Hamiltonian (1) with $R = 3$, 4, 5, and 6 as shown in Fig. 8. Moreover, the critical transition points of the $(R + 1)$-mer hole substaircase and the $(R + 2)$-mer hole substaircase to the fully filled $f = 1$ particle states can also be found from Eq. (8).

VI. $N(\geqslant 3)$-BODY INTERACTION DRIVEN STAIRCASE

The above results indicate that there should be an R-mer staircase when the range of the attractive interactions is $R - 1$. A natural question is whether such an R-mer staircase can be induced by R-body interactions directly? To answer this question, we investigate the following model Hamiltonian, which contains a two-body long-range repulsive interaction described by $V(r)$, and an $N \geqslant 3$-body attractive interaction
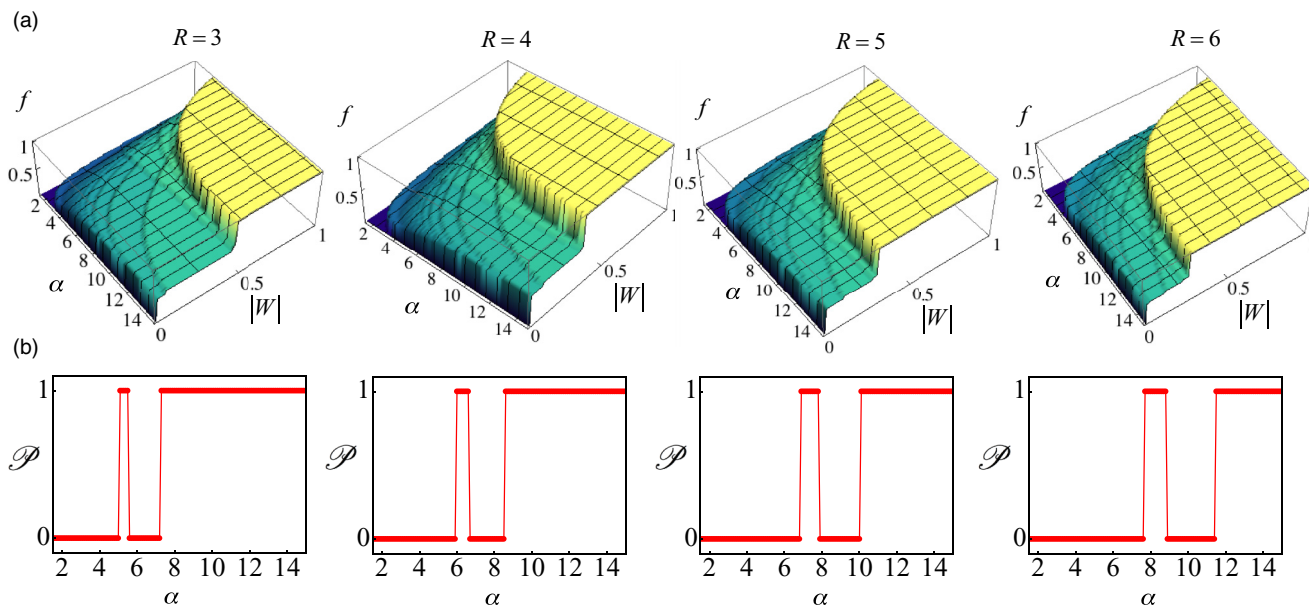

FIG. 8. (a) Ground-state filling fraction f of Hamiltonian (1) for $R = 3$, 4, 5, 6 shown as a function of the attractive interaction strength $W(i) = W$ $(i = 1, 2, \ldots, R)$ and the power α of the long-range power law repulsion $V(r) = (R + 1)^{\alpha}/r^{\alpha}$ with $(r = R + 1, \ldots)$. Shown in (b) is $\mathscr{P}(\alpha)$ similar to Figs. 4(b) and 6(b) at $R = 1$ and $R = 2$.

by U_N,

$$H = \sum_{i=-\infty}^{\infty} \sum_{r=1}^{\infty} V(r) n_i n_{i+r} - U_N \sum_{i=-\infty}^{\infty} n_i n_{i+1} \cdots n_{i+N-1}.$$

(23)

Numerical calculations of the above Hamiltonian show that in the ground state, there is always a direct transition from the empty state of $\ldots 000 \ldots$ to the fully filled state of $\ldots 111 \ldots$. The energies of the two states are 0 and $\sum_{r \geqslant 1} V(r) - U_N$. Hence the transition happens when $[\sum_{r \geqslant 1} V(r) - U_N] < 0$, i.e., $U_N > \sum_{r \geqslant 1} V(r) = \zeta(\alpha)$.

In the following, we provide a simple explanation of this result based on energy arguments. The energy of an N-mer is

$$E_N = (N-1)V(1) + (N-2)V(2) + \cdots V(N-1) - U_N.$$

One can readily show that the energy of two separate N-mers are $2E_N + E_{\text{int}}$, with E_{int} the interaction energy of the two N-mers, which is larger than the energy of an $(N+1)$-mer,

$$\begin{aligned} 2E_N &+ E_{\text{int}} - E_{N+1} \\ &= (N-2)V(1) + (N-3)V(2) + \cdots \\ &\quad + (-1)V(N) + E_{\text{int}} > 0, \end{aligned}$$

when $N \geqslant 3$. This result excludes the possibility of having exotic staircases driven solely by N-body attraction when $N \geqslant 3$.

VII. DISCUSSION AND OUTLOOK

We have explored a different class of devil's staircases that exhibits a broken particle-hole symmetry. The symmetry breaking is purely induced by the interplay between short-range attraction and long-range repulsion. When the staircase can be described by a union of two pure substaircases in both the particle and hole sectors, the value of the critical attractive strength W_c and the "width" of the stability region can be found analytically. These confirm that the resulting staircase is complete [8,35]. However, when the staircase contains mixtures of n-mers of different kinds, it is an open question whether an analytic understanding of the staircase structure can be obtained. Another possible way to understand the problem—which may lead to an answer—is to consider periodic configurations as consisting of segments of different phases separated by interfaces [53], where the nature of the interface interactions determines the detailed structure of the phase diagram. One interesting question is why, for attractive interactions with range R, there can only be $(R+1)$-mer hole and $(R+2)$-mer hole substaircases but not an $(R+3)$ hole substaircase in the hole sector for power-law repulsion. The answer might be that without particle-hole symmetry, the staircase structure will depend on the specific form of the repulsive tail itself. This also suggests an interesting way to manipulate the hole part of the staircase by controlling the form of the repulsive tail. We expect that, for example, with exponential interactions [54] for the repulsive part, the hole part may indeed display a different structure. Furthermore, it is known that some two-dimensional (2D) lattice gas [55] and adsorption [56] models can have a devil's staircase of phase transitions in the ground state. So it would be interesting

to extend the current work to 2D by coupling 1D chains transversely.

A further interesting problem for future studies is the exploration of the role of thermal and quantum fluctuations. For example, for the ANNNI model, it is the thermal fluctuations that stabilize the staircase. Quantum fluctuations, however, can destroy the staircase at zero temperature [35,57,58], i.e., the stability regions shrink and at most a finite number of commensurate phases survives. So it would be interesting to understand how quantum fluctuations will melt the emerging hybrid staircases, such as the dimer-particle and trimer-hole staircase [see Fig. 5(c)] studied in this paper. One might be able to address these questions experimentally, for example, with a recently established quantum simulator platform based on Rydberg atoms [30,59–61]. The preparation of the ground state of our model on a Rydberg atom quantum simulator requires an adiabatic sweep protocol. A detailed discussion of this procedure can be found in the recent review [61].

APPENDIX A: STABILITY REGIONS

In this Appendix, we give a brief derivation of the stability regions of Eqs. (3) and (4) used in the main text (see Refs. [51,52] for the original literature). The energy of the ground-state configuration can be written as

$$E_0 = E_1 + E_2 + \cdots + E_n + \cdots + E_\infty + E_\mu,$$

where $E_{1,2,\ldots,\infty}$ is the interaction energy with nearest-neighbor and next-nearest-neighbor and so on and E_μ is the energy with the chemical potential term. For any filling fraction of $f = \frac{q}{p}$, the n-nearest-neighbor interaction energy of the most homogeneous configuration requires $np = r_n q + \alpha_n$, where $0 \leqslant \alpha_n < q$. To make this relation clear, we rewrite it as $np = r_n x + (r_n + 1)(q - x)$ by introducing a new integer $x = (r_n + 1)q - np$. It means that there are x particles separated from each other by r_n lattice sites while $q - x$ particles separated from each other by $r_n + 1$ lattice sites. The energy of E_n with L periods (a very large number) is then

$$E_n = [x V(r_n) + (q - x) V(r_n + 1)]L.$$

Now if we have one more particle in the above configuration, the interaction will reorganize the particle distribution such that $npL = r_n y + (qL + 1 - y)(r_n + 1)$, i.e., compared with the above case, we have $qL + 1$ particles, from which we can get $y = (qL + 1)(r_n + 1) - npL$, so the energy of E_n^+ with
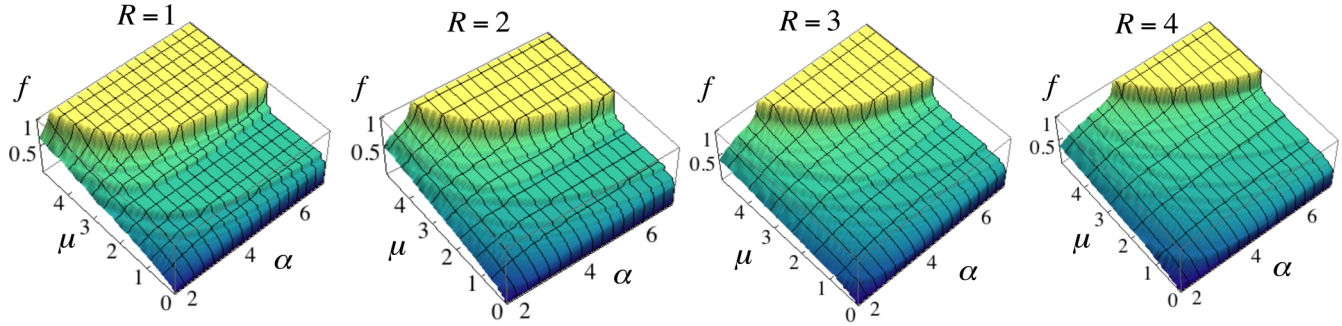
FIG. 9. Ground-state filling fraction f of Hamiltonian (2) for $R = 1, 2, 3, 4$ as functions of the chemical potential μ and the power α of the long-range power-law repulsion $V(r) = R^\alpha/r^\alpha$ $(r = R + 1, \ldots)$, where the short-range attractions $W(i)$ $(i = 1, 2, \ldots, R)$ have been set to zero. This chemical potential μ driven staircase has the particle-hole symmetry, so the hole sector is trivially related to the particle sector, which is very different from our two-body attraction $W(i)$ driven staircase, where the hole sector contains very rich physics, as studied in the main text.

one more particle is

$$E_n^+ = yV(r_n) + (qL + 1 - y)V(r_n + 1).$$

In the same way for one less particle in the configuration, $npL = r_n z + (qL - 1 - z)(r_n + 1)$, and we get $z = (qL - 1)(r_n + 1) - npL$ and

$$E_n^- = zV(r_n) + (qL + 1 - z)V(r_n + 1).$$

However, if $\alpha_n = 0$, i.e., $x = q$, we have slightly different situations,

$$E_n = [qV(r_n)]L,$$
$$E_n^+ = yV(r_n) + (qL + 1 - y)V(r_n - 1),$$
$$E_n^- = zV(r_n) + (qL - 1 - z)V(r_n + 1),$$
$$r_n y + (qL + 1 - y)(r_n - 1)$$
$$= npL \Rightarrow y = npL - (qL + 1)(r_n - 1),$$
$$r_n z + (qL - 1 - z)(r_n + 1)$$
$$= npL \Rightarrow z = (qL - 1)(r_n + 1) - npL.$$

In summary, we get

$$\mu^+ = \sum_{n=1, \alpha_n \neq 0}^{\infty} (E_n^+ - E_n)$$

$$= \sum_{n=1, \alpha_n \neq 0}^{\infty} [(r_n + 1)V(r_n) - r_n V(r_n + 1)]$$

$$+ \sum_{n, \alpha_n = 0}^{\infty} [(-r_n + 1)V(r_n) + r_n V(r_n - 1)]$$

and

$$\mu^- = \sum_{n=1, \alpha_n \neq 0}^{\infty} (E_n - E_n^-)$$

$$= \sum_{n=1, \alpha_n \neq 0}^{\infty} [(r_n + 1)V(r_n) - r_n V(r_n + 1)]$$

$$+ \sum_{n, \alpha_n = 0}^{\infty} [(r_n + 1)V(r_n) - r_n V(r_n + 1)],$$

which are used in the main text.

APPENDIX B: POLYMER STAIRCASES WITH PARTICLE-HOLE SYMMETRY

In the main text, we study the devil's staircase physics described by Hamiltonian (1) where the short-range two-body attraction is the main driving force for the emergence of devil's staircase behavior. The emergent staircases could be termed as polymer staircases, which consist of some basic clusters with different sizes. Our main motivation of the main text is to study the effect of broken particle-hole symmetry on the staircase structure where the polymer behavior of the staircases is a by-product. However, we note that in the literature there have been studies where the motivation was to look for a mechanism to form a polymer staircase, whereas the particle-hole symmetry is not the focus. Actually, one can still preserve the particle-hole symmetry of the polymer staircases by using the single-body chemical potential as the driven mechanism, e.g., the papers by Jedrzejewski and Miekisz [62,63] fit to this category.

Here, we would like to briefly discuss the connection of our work with those of Jedrzejewski and Miekisz [62,63]. These authors have proven rigorously the existence of the dimer staircases in 1D lattice gas models with certain nonconvex long-range interactions, where the particle density versus the chemical potential $\rho(\mu)$ exhibits the complete devil's staircase structure. The authors also speculated that for interactions with values near zero for distances up to R and strictly convex from distance $R + 1$ onwards, the ground state forms an $R + 1$-mer staircase. We present in Fig. 9 the staircase structure according to the speculation of the papers by Jedrzejewski and Miekisz [62,63] using the numerical tool described in our main text, where we set $W(1) = \cdots W(R) = 0$, and from distance $R + 1$ onwards, the repulsive interaction has the form of $(R + 1)^\alpha/r^\alpha$. From the numerical results, we verify that given R, the staircase is an $(R + 1)$-mer staircase with exact particle-hole symmetry [see Fig. 9, where the mesa is symmetric with respect to the $f = 1/2$ plateaus possessing a configuration of $(1 \ldots 10 \ldots 0) \ldots$ with both $R + 1$ "1"s and $R + 1$ "0"s in one period]. Due to the particle-hole symmetry, the hole sectors of these staircases are trivially related to the particle sectors of them. This kind of staircase bears some similarities with both the traditional staircases presented in Sec. IV and our two-body attraction driven staircases studied in Sec. V in the sense that they have particle-hole symmetry as the traditional staircases but show cluster behavior as our two-body attraction driven staircases.

[1] P. Bak, Commensurate phases, incommensurate phases and the devil's staircase, Rep. Prog. Phys. **45**, 587 (1982).

[2] P. Bak, The devil's staircase, Phys. Today **39**(12), 38 (1986).

[3] O. M. Braun and Y. Kivshar, *The Frenkel-Kontorova Model: Concepts, Methods, and Applications* (Springer, Berlin, 2004).

[4] S. Aubry, Exact models with a complete devil's staircase, J. Phys. C: Solid State Phys. **16**, 2497 (1983).

[5] G. I. Watson and R. Lemanski, The ground-state phase diagram of the two-dimensional Falicov-Kimball model, J. Phys.: Condens. Matter **7**, 9521 (1995).

[6] C. Micheletti, A. B. Harris, and J. M. Yeomans, A complete devil's staircase in the Falicov-Kimball model, J. Phys. A: Math. Gen. **30**, L711 (1997).

[7] P. Farkasovsky, Ground-state properties of the Falicov-Kimball model in one and two dimensions, Eur. Phys. J. B **20**, 209 (2001).

[8] P. Bak and R. Bruinsma, One-Dimensional Ising Model and the Complete Devil's Staircase, Phys. Rev. Lett. **49**, 249 (1982).

[9] P. Bak and J. von Boehm, Ising model with solitons, phasons, and "the devil's staircase," Phys. Rev. B **21**, 5297 (1980).

[10] E. Fradkin, D. A. Huse, R. Moessner, V. Oganesyan, and S. L. Sondhi, Bipartite Rokhsar-Kivelson points and Cantor deconfinement, Phys. Rev. B **69**, 224415 (2004).

[11] A. Vishwanath, L. Balents, and T. Senthil, Quantum criticality and deconfinement in phase transitions between valence bond solids, Phys. Rev. B **69**, 224416 (2004).

[12] S. Papanikolaou, K. S. Raman, and E. Fradkin, Devil's staircases, quantum dimer models, and stripe formation in strong coupling models of quantum frustration, Phys. Rev. B **75**, 094406 (2007).

[13] M. H. Jensen, P. Bak, and T. Bohr, Complete Devil's Staircase, Fractal Dimension, and Universality of Mode-Locking Structure in the Circle Map, Phys. Rev. Lett. **50**, 1637 (1983).

[14] A. Jazaeri and I. I. Satija, Double devil's staircase in circle maps, Phys. Rev. A **46**, 737 (1992).

[15] S.-X. Qu, S. Wu, and D.-R. He, Multiple devil's staircase and type-V intermittency, Phys. Rev. E **57**, 402 (1998).

[16] K. Ohwada, Y. Fujii, N. Takesue, M. Isobe, Y. Ueda, H. Nakao, Y. Wakabayashi, Y. Murakami, K. Ito, Y. Amemiya, H. Fujihisa, K. Aoki, T. Shobu, Y. Noda, and N. Ikeda, "Devil's Staircase"-Type Phase Transition in NaV_2O_5 under High Pressure, Phys. Rev. Lett. **87**, 086402 (2001).

[17] I. M. Georgescu, S. Ashhab, and F. Nori, Quantum simulation, Rev. Mod. Phys. **86**, 153 (2014).

[18] P. Hauke, F. M. Cucchietti, A. Múller-Hermes, M.-C. Bañuls, J. I. Cirac, and M. Lewenstein, Complete devil's staircase and crystal-superfluid transitions in a dipolar XXZ spin chain: A trapped ion quantum simulation, New J. Phys. **12**, 113037 (2010).

[19] P. Richerme, C. Senko, S. Korenblit, J. Smith, A. Lee, R. Islam, W. C. Campbell, and C. Monroe, Quantum Catalysis of Magnetic Phase Transitions in a Quantum Simulator, Phys. Rev. Lett. **111**, 100506 (2013).

[20] F. J. Burnell, M. M. Parish, N. R. Cooper, and S. L. Sondhi, Devil's staircases and supersolids in a one-dimensional dipolar Bose gas, Phys. Rev. B **80**, 174519 (2009).

[21] M. Knap, E. Berg, M. Ganahl, and E. Demler, Clustered Wigner-crystal phases of cold polar molecules in arrays of one-dimensional tubes, Phys. Rev. B **86**, 064501 (2012).

[22] M. Bauer and M. M. Parish, Dipolar Gases in Coupled One-Dimensional Lattices, Phys. Rev. Lett. **108**, 255302 (2012).

[23] B. Capogrosso-Sansone, C. Trefzger, M. Lewenstein, P. Zoller, and G. Pupillo, Quantum Phases of Cold Polar Molecules in 2D Optical Lattices, Phys. Rev. Lett. **104**, 125301 (2010).

[24] L. Pollet, J. D. Picon, H. P. Büchler, and M. Troyer, Supersolid Phase with Cold Polar Molecules on a Triangular Lattice, Phys. Rev. Lett. **104**, 125302 (2010).

[25] H. Weimer and H. P. Büchler, Two-Stage Melting in Systems of Strongly Interacting Rydberg Atoms, Phys. Rev. Lett. **105**, 230403 (2010).

[26] A. Lauer, D. Muth, and M. Fleischhauer, Transport-induced melting of crystals of Rydberg dressed atoms in a one-dimensional lattice, New J. Phys. **14**, 095009 (2012).

[27] E. Sela, M. Punk, and M. Garst, Dislocation-mediated melting of one-dimensional Rydberg crystals, Phys. Rev. B **84**, 085434 (2011).

[28] A. Geißler, I. Vasić, and W. Hofstetter, Condensation versus long-range interaction: Competing quantum phases in bosonic optical lattice systems at near-resonant Rydberg dressing, Phys. Rev. A **95**, 063608 (2017).

[29] T. Pohl, E. Demler, and M. D. Lukin, Dynamical Crystallization in the Dipole Blockade of Ultracold Atoms, Phys. Rev. Lett. **104**, 043002 (2010).

[30] P. Schauß, J. Zeiher, T. Fukuhara, S. Hild, M. Cheneau, T. Macrì, T. Pohl, I. Bloch, and C. Gross, Crystallization in Ising quantum magnets, Science **347**, 1455 (2015).

[31] S. Li, I. I. Satija, C. W. Clark, and A. M. Rey, Exploring complex phenomena using ultracold atoms in bichromatic lattices, Phys. Rev. E **82**, 016217 (2010).

[32] T. Y. Saito and S. Furukawa, Devil's staircases in synthetic dimensions and gauge fields, Phys. Rev. A **95**, 043613 (2017).

[33] Y. Zhang, J. Fan, J.-Q. Liang, J. Ma, G. Chen, S. Jia, and F. Nori, Photon devil's staircase: photon long-range repulsive interaction in lattices of coupled resonators with Rydberg atoms, Sci. Rep. **5**, 11510 (2015).

[34] H. Wang, Y. Dhayalan, and E. Buks, Devil's staircase in an optomechanical cavity, Phys. Rev. E **93**, 023007 (2016).

[35] Z. Lan, J. Minář, E. Levi, W. Li, and I. Lesanovsky, Emergent Devil's Staircase without Particle-Hole Symmetry in Rydberg Quantum Gases with Competing Attractive and Repulsive Interactions, Phys. Rev. Lett. **115**, 203001 (2015).

[36] S. Aubry, K. Fesser, and A. R. Bishop, Locking to incommensurate structures—a model with three competing lengths, J. Phys. A: Math. Gen. **18**, 3157 (1985).

[37] N. Ishimura, A devil's staircase and the ground state phase diagram in an Ising chain with spin-lattice coupling, J. Phys. Soc. Jpn. **54**, 4752 (1985).

[38] N. Ishimura and T. Yamamoto, Commensurate structures of adatoms on a square lattice, J. Phys. Soc. Jpn. **58**, 2439 (1989).

[39] K. Sasaki, Modulated phases and Upsilon poins in a spin model with helical ordering, J. Stat. Phys. **68**, 1013 (1992).

[40] K. Sasaki, Lattice gas model for striped structures of adatom rows on surfaces, Surf. Sci. **318**, L1230 (1994).

[41] K. E. Bassler and R. B. Griffiths, Numerical study of a new type of nonconvex Frenkel-Kontorova model, Phys. Rev. B **49**, 904 (1994).

[42] C. Micheletti, F. Seno, and J. M. Yeomans, Upsilon point in a spin model, Phys. Rev. B **52**, 4353 (1995).

[43] K. Sasaki, Exact renormalization analysis of a self-similar phase diagram with upsilon points for an Ising model, J. Phys. Soc. Jpn. **68**, 3562 (1999).

[44] B. Olmos, W. Li, S. Hofferberth, and I. Lesanovsky, Amplifying single impurities immersed in a gas of ultracold atoms, Phys. Rev. A **84**, 041607(R) (2011).

[45] N. Henkel, R. Nath, and T. Pohl, Three-Dimensional Roton Excitations and Supersolid Formation in Rydberg-Excited Bose-Einstein Condensates, Phys. Rev. Lett. **104**, 195302 (2010).

[46] J. Honer, H. Weimer, T. Pfau, and H. P. Büchler, Collective Many-Body Interaction in Rydberg Dressed Atoms, Phys. Rev. Lett. **105**, 160404 (2010).

[47] F. Cinti, P. Jain, M. Boninsegni, A. Micheli, P. Zoller, and G. Pupillo, Supersolid Droplet Crystal in a Dipole-Blockaded Gas, Phys. Rev. Lett. **105**, 135301 (2010).

[48] W. Li, L. Hamadeh, and I. Lesanovsky, Probing the interaction between Rydberg-dressed atoms through interference, Phys. Rev. A **85**, 053615 (2012).

[49] C. Ates, B. Olmos, W. Li, and I. Lesanovsky, Dissipative Binding of Lattice Bosons through Distance-Selective Pair Loss, Phys. Rev. Lett. **109**, 233003 (2012).

[50] W. Li, C. Ates, and I. Lesanovsky, Nonadiabatic Motional Effects and Dissipative Blockade for Rydberg Atoms Excited from Optical Lattices or Microtraps, Phys. Rev. Lett. **110**, 213005 (2013).

[51] J. Hubbard, Generalized Wigner lattices in one dimension and some applications to tetracyanoquinodimethane (TCNQ) salts, Phys. Rev. B **17**, 494 (1978).

[52] V. L. Pokrovsky and G. V. Uimin, On the properties of monolayers of adsorbed atoms, J. Phys. C: Solid State Phys. **11**, 3535 (1978).

[53] K. E. Bassler, K. Sasaki, and R. B. Griffiths, Interface interactions in modulated phases, and upsilon points, J. Stat. Phys. **62**, 45 (1991).

[54] R. J. Krantz, J. Douthett, and S. D. Doty, Maximally even sets and the devil's-staircase phase diagram for the one-dimensional Ising antiferromagnet with arbitrary-range interaction, J. Math. Phys. **39**, 4675 (1998).

[55] Yu. I. Dublenych, Ground states of lattice-gas models on the triangular and honeycomb lattices: Devil's step and quasicrystals, Phys. Rev. E **80**, 011123 (2009).

[56] V. F. Fefelov, V. A. Gorbunov, A. V. Myshlyavtsev, M. D. Myshlyavtseva, and S. S. Akimenko, Devil's staircase behavior of a dimer adsorption model, Adsorption **19**, 495 (2013).

[57] P. Bak, Destruction of "the devil's staircase" by quantum fluctuations, Phys. Rev. B **21**, 3287 (1980).

[58] Z. Lan, W. Li, and I. Lesanovsky, Quantum melting of two-component Rydberg crystals, Phys. Rev. A **94**, 051603(R) (2016).

[59] H. Labuhn, D. Barredo, S. Ravets, S. de Léséleuc, T. Macrì, T. Lahaye, and A. Browaeys, Tunable two-dimensional arrays of single Rydberg atoms for realizing quantum Ising models, Nature (London) **534**, 667 (2016).

[60] H. Bernien, S. Schwartz, A. Keesling, H. Levine, A. Omran, H. Pichler, S. Choi, A. S. Zibrov, M. Endres, M. Greiner, V. Vuletić, and M. D. Lukin, Probing many-body dynamics on a 51-atom quantum simulator, Nature (London) **551**, 579 (2017).

[61] P. Schauss, Quantum simulation of transverse Ising models with Rydberg atoms, Quantum Sci. Technol. **3**, 023001 (2018).

[62] J. Jedrzejewski and J. Miekisz, Devil's staircase for nonconvex interactions, Europhys. Lett. **50**, 307 (2000).

[63] J. Jedrzejewski and J. Miekisz, Ground states of lattice gases with "almost" convex repulsive interactions, J. Stat. Phys. **98**, 589 (2000).